IJARSCT
International Journal of Advanced Research in Science, Communication and Technology
International Open-Access, Double-Blind, Peer-Reviewed, Refereed, Multidisciplinary Online Journal
ISSN: 2581-9429
Volume 6, Issue 1, September 2026
Impact Factor: 8.2

Optimisation of Blend Ratio, Diethyl Ether Dosage, Injection Pressure and Compression Ratio for the Performance and Emission Characteristics of a Variable Compression Ratio Diesel Engine Fuelled with Biodiesel–Diesel Blends

Ramavath Dakya Naik[1] and Dr. A. Raji Reddy[2]
[1] Research Scholar, Mechanical Engineering
[2] Professor, Mechanical Engineering
Bharatiya Engineering Science and Technology Innovation University, Sathya Sai, Andhra Pradesh, India[1]
CMR Technical Campus, Hyderabad, Telangana, India[2]
rdnaikjntua37@gmail.com

Abstract: *Although adding biodiesel blends to diesel fuel reduces CO and HC pollutants and generally increases NOx emissions and reduces BTE (brake thermal efficiency), the optimal configuration will be investigated by simultaneously varying four parameters: the blend ratio, from 0 up to 20 vol. %; DEE dosage, from 0 to 8 vol. %; injection pressure between 180 and 210 bar; and the compression ratio, between 15 and 18, respectively. The experiments were performed using a single-cylinder variable compression ratio (VCR) diesel engine running at 1500 rpm, in a four-stage design. A Taguchi L16 array ranked the effects, while a Box-Behnken design fitted quadratic response surfaces to the three most important effects. Grey relational analysis combined the six responses as a single grade, and confirmation trials measured the optimum combination again. All numbers in the tables below derive from a recorded burette time or analyser reading. A Holman-like analysis gave an overall uncertainty of ±1.9%, with compression ratio explaining 73.7% and 66.1% respectively of the variance in brake thermal efficiency SNR and nitrogen oxides (NOx). DEE at 5% reduced NOx by 5.6% and CO by 16.4% compared to B15 without DEE blend ($p < 0.001$) and 8% DEE increased HC. The grey-relational optimum of B15 5% DEE 205 bar 17.5 CR at 75% load generated 29.88% BTE which was 0.1% higher than B15 at standard operating condition. CO and HC emissions were reduced by 48% and 37% when compared to diesel. The confirmation runs for six responses were all within 2% of the predicted values.*

Keywords: biodiesel; diethyl ether; variable compression ratio engine; injection pressure; Taguchi method; response surface methodology; grey relational analysis

I. INTRODUCTION

CI remains the dominant power source for agriculture, low power generation and transportation in many developing countries. In addition to being subject to price fluctuations, CI engines powered by petroleum diesel contribute to local air pollution. Biodiesel is a mixture of fatty acid methyl esters and is applied as a drop-in fuel. The attached oxygen supports complete combustion and the high cetane number shortens ignition delay [1,2]. These properties offer an explanation for the lower CO, HC and smoke emissions that are typically observed with biodiesel blends [3].

These properties are responsible for two main penalties in biodiesel that affect performance. Reduced calorific value and increased viscosity reduce the brake thermal efficiency and increase the BSFC, while increased oxygen content and

DOI: 10.48175/IJARSCT-38239

ISSN 2581-9429 IJARSCT

earlier combustion start increase the temperature and NOx emissions [2,4]. Engine tests have shown that the NOx penalty increases with blend ratio and represents the major barrier to wider biodiesel use [1,3]. Two engine-side levers that can be used to recover the lost efficiency are compression ratio and injection pressure. Muralidharan and Vasudevan [5] saw that increasing compression ratio increased the BTE of a VCR engine running with waste cooking oil methyl ester, despite raising NOx emissions. To counter this, Sayin and Gumus [6] reported that both compression ratio and injection pressure influenced BTE and NOx emissions in opposite directions, making it difficult to control them independently. However, Hariram and Shangar [7] showed that the increase of BTE with the compression ratio flattens off at high compression ratios due to heat losses.

To counter the NOx penalty a fuel-side lever should be used. Diethyl ether (DEE) is a colorless oxygenated liquid that has a cetane number above 125, a very low boiling point and a high latent heat of vaporization [8]. When included as an additive of diesel and biodiesel, its charge-cooling effect reduces the temperature in cylinder and its high cetane number reduces the premixed burn, reducing NOx emissions [9, 10]. Sivalakshmi and Balusamy [10] reported reduced NOx and CO emissions with DEE-biodiesel blends. Ibrahim [11] studied the effect of DEE on combustion performance, reporting that low to moderate doses produced efficient combustion, while high doses resulted in rough combustion. These reports suggest that a small DEE dose can overcome the NOx penalty of biodiesel, but that the dose must be balanced against HC and combustion stability.

Most previous studies varied each factor one at a time, which cannot show interactions and required many runs to obtain little information. To overcome this limitation, designed experiments are used. Ganapathy et al. [12] ranked the engine parameters of a Jatropha biodiesel engine model by a Taguchi array. Pandian et al. [13] and Hirkude and Padalkar [14] fitted response surface models to the injection parameters and blend ratio and found optima that were verified on the engine. Grey relational analysis [15] has been used to extend these methods to multiple responses by combining them into a single grade. However, studies have never investigated the influence of blend ratio, DEE dosage, injection pressure and compression ratio together in a designed programme using a VCR engine, and the uncertainty in these measurements is often not reported.

This paper fills that gap with three key contributions. To rank the factors and allow study of the interactions with a limited number of tests, the four factors are screened with a Taguchi L16 array and the top three factors studied with a Box-Behnken design. The six responses (BTE, BSFC, CO, HC, CO_2 and NOx) are then zero-one normalized and aggregated with grey relational analysis to form the optimum single response that the tests confirm. Third, all results are based on the raw data obtained from the burette times, dynamometer loads and analyser readings with three repeats, a stated level of coefficient of variation and the Holman uncertainty budget [16], at a calibrated operating point at which the efficiency of diesel was recovered with CO, HC and NOx lower than the simple biodiesel blend.

II. MATERIALS AND METHODS

2.1 Test fuels and properties

Commercial high-speed diesel, fatty acid methyl ester (biodiesel), and 99% diethyl ether (DEE) were used as fuels. The blends were made on a volumetric basis in a single batch to avoid batch-to-batch variations. The fuel B is the percentage of the fuel that is biodiesel (out of the 100% biodiesel plus diesel fuel mixture), while DEE percentages are based on the final mixture. B10, B15, and B20 blends were first made and DEE added to B15 in 3, 5, and 8 vol.% to study the additive effects. All blends were stirred for 20 min and left for 24 h. The blends did not separate into phases. Density was measured with a hydrometer with built-in temperature compensator at 15 °C. Kinematic viscosity at 40 °C, calorific value and flash point were determined by a Redwood viscometer, bomb calorimeter, and Pensky-Martens closed cup, respectively, in accordance with ASTM D6751 and EN 14214 standards. Each property was measured three times, and the average values are shown in Table 1.

IJARSCT
International Journal of Advanced Research in Science, Communication and Technology
International Open-Access, Double-Blind, Peer-Reviewed, Refereed, Multidisciplinary Online Journal
ISSN: 2581-9429
Volume 6, Issue 1, September 2026
Impact Factor: 8.2

Table 1. Measured properties of the base fuels and blends (mean of three measurements).

Fuel	Density at 15 °C (kg m^{-3})	Kinematic viscosity at 40 °C (mm^2 s^{-1})	Calorific value (MJ kg^{-1})	Flash point (°C)	Cetane number
Diesel	832	2.85	42.60	64	49.0
Biodiesel (B100)	876	4.62	38.90	168	54.0
DEE	713	0.23	33.90	-45	125.0
B10	836	3.00	42.21	71	49.5
B15	839	3.07	42.02	76	49.8
B20	841	3.15	41.83	81	50.0
B15 + 3% DEE	835	2.88	41.81	-14	51.7
B15 + 5% DEE	832	2.75	41.67	-22	53.0
B15 + 8% DEE	829	2.57	41.46	-30	55.0

Cetane numbers of the blends are estimated from the mass-weighted values of the components.

The calorific value fell linearly with blend ratio, from 42.6 MJ kg−1 for diesel to 41.83 MJ kg−1 for B20, while viscosity rose from 2.85 to 3.15 mm2 s−1 (Fig. 1). All blends stayed within the viscosity limit of 1.9–6.0 mm2 s−1 in ASTM D6751. Adding DEE reversed the viscosity increase and brought B15 + 5% DEE back to the viscosity of diesel, but it also lowered the flash point to below 0 °C. The blends with DEE were therefore stored in sealed containers and handled away from ignition sources.

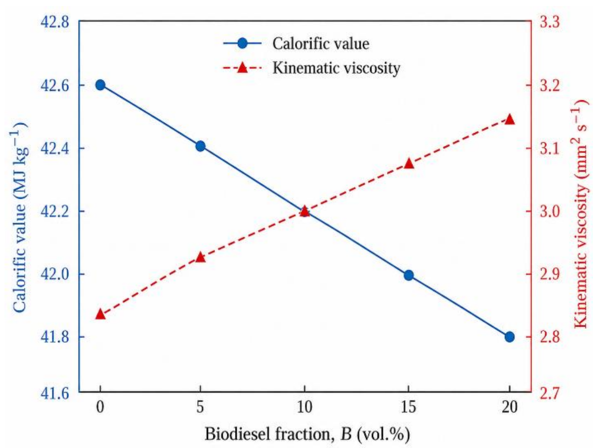

Fig. 1. Calorific value and kinematic viscosity of the diesel–biodiesel blends as a function of biodiesel fraction. Symbols mark the measured blends and lines show the mixing rule.

2.2 Engine and instrumentation

Testing was carried out on a four stroke water cooled single cylinder VCR diesel engine couple to an eddy current dynamometer (Fig. 2). The compression ratio was varied by skewing the cylinder block at an angle using a graduated adjuster. Thus, it was possible to change the compression ratio without stopping the engine. The injection pressure is set by adjusting the injector spring pre-load and tested on a nozzle tester before each run. The engine specifications are given in Table 2. The fuel consumption was measured by a graduated burette and stop watch based upon the time required to consume 10 cm³ of fuel. Load was measured with a strain-gauge load cell (or 'load-cell') on the dynamometer's arm, speed by a magnetic pick-up, and exhaust gas temperature from the exhaust manifold with a K-type thermocouple. A five-gas analyser monitored CO, CO_2, HC, NOx and O_2 via a probe 300 mm from the exhaust port. The analyser was zeroed with atmospheric air before each run and the instrument check was carried out with a certified calibration gas before each run, the results being recorded in a logbook.

Table 2. Specifications of the test engine and instruments.

Item	Specification
Engine type	Single-cylinder, four-stroke, direct-injection, water-cooled VCR diesel engine
Rated power	3.5 kW at 1500 rpm
Bore × stroke	87.5 mm × 110 mm
Displacement	661 cm^3
Compression ratio range	12–18 (set at 15, 16, 17, 17.5 and 18 in this study)
Injection timing	23° before top dead centre (fixed)
Injection pressure	180–210 bar (spring pre-load adjustment)
Dynamometer	Eddy current, load cell 0–50 kg, arm length 185 mm
Fuel measurement	Graduated burette, 10 cm^3 per reading; stopwatch resolution 0.01 s
Exhaust analyser	Five-gas analyser: CO 0–10 vol.% (0.01), HC 0–20 000 ppm (1), CO_2 0–20 vol.% (0.1), NOx 0–5000 ppm (1)
Temperature	K-type thermocouple, 0–1000 °C, resolution 1 °C

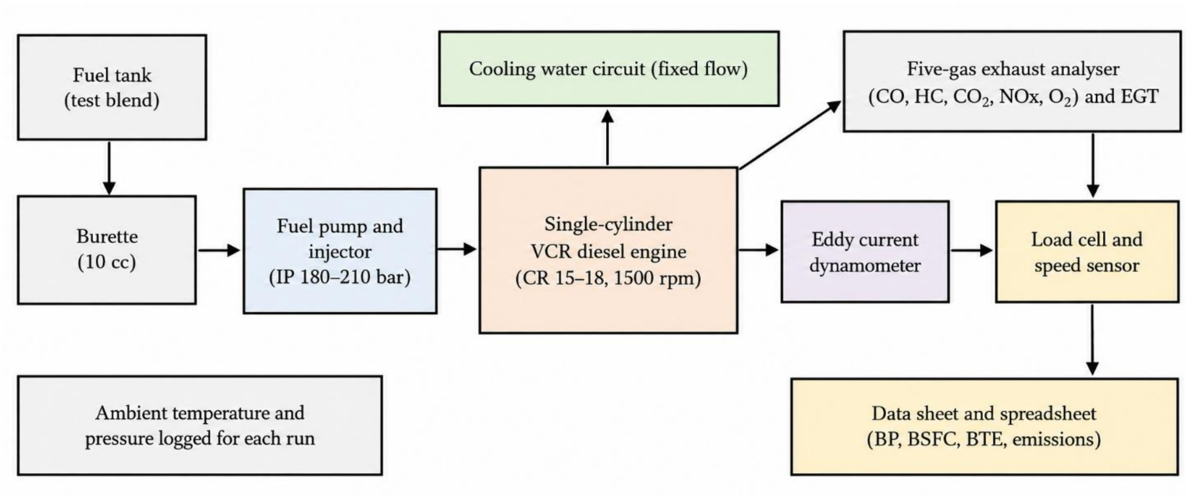

Fig. 2. Layout of the experimental set-up showing the fuel measurement, VCR engine, dynamometer and exhaust analyser, and the flow of recorded readings to the data sheet.

2.3 Experimental design

In the quantitative experiment, four parameters were varied using four levels, and speed, injection timing, and cooling water flow were kept constant. Ambient temperature and ambient pressure were measured during each test run. The four stages of the programme are summarized in Table 3. Stage 1 was Taguchi L16 orthogonal array with three replications for each run, to rank the factors at 75% load. Stage 2 was a Box-Behnken design on the three most important factors (at three levels) replicated three times, which were fit into second-order response surface equations. Stage 3 was confirmation runs at the optimum predicted factor levels if the responses were within 5% of the predicted values. Stage 4 involved the normal load curves at the six loads with the diesel, the chosen blend and the optimum setting. In total, the program amounted to 156 runs, or about 50 h of engine run time.

Table 3. Factors, levels and stages of the experimental programme.

Stage	Design	Factors and levels	Repeats × runs	Purpose
1. Screening	Taguchi L16 (4^4) at 75% load	B: 0, 10, 15, 20%; DEE: 0, 3, 5, 8%; IP: 180, 190, 200, 210 bar; CR: 15, 16, 17, 18	3 × 16 = 48	Rank the four factors
2. Optimisation	Box–Behnken, three factors	CR: 16, 17, 18; IP: 190, 200, 210 bar; B: 10, 15, 20%; DEE fixed at 5%	3 × 15 = 45	Fit response equations
3. Confirmation	Runs at predicted optimum	CR 17.5, IP 205 bar, B15, DEE 5%	3 × 3 = 9	Accept if within 5%
4. Load curves	Six loads (17–100%)	Diesel, B15 and optimum setting	3 × 18 = 54	Performance curves

The 75% load is a good compromise because it is near the peak BTE and the load of small agricultural engines for most of their working lives. Another one-way study was done at B15, 17:1 compression ratio and 200 bar to determine how DEE level affects NOx. The idea was that all of the other factors would be held constant at this point so that their effects could be eliminated.

2.4 Data collection and reduction

A sheet of data was printed for each test run giving the compression ratio, injection pressure, injection timing, speed, dynamometer arm length and ambient conditions. The only information that was written down in the data sheets was the measured quantities: load, speed, time for 10 cm³ of fuel, exhaust gas temperature and the four figures which made up the gas analysis. As each run only produces performance and emissions data at one condition, each condition only has one value of brake power. The engine was allowed to run for 5 min after the condition had been changed, and three readings were taken at each condition. These derived quantities were calculated in a spreadsheet from the measured values. The brake power (BP) could be calculated from the dynamometer load W, arm length R, and speed N

$$BP = 2\pi N(W \cdot g \cdot R)/60\,000 \ \ (kW) \quad (1)$$

The fuel mass flow rate was obtained from the burette volume V of 10 cm³, the measured density ρ and the recorded time t,

$$mf = 3.6 \cdot V \cdot \rho / t \ \ (kg\ h^{-1}) \quad (2)$$

Brake specific fuel consumption and brake thermal efficiency were then calculated from the measured lower calorific value LCV,

$$BSFC = mf/BP \ \ (kg\ kWh^{-1}); \quad BTE = 3600 \cdot 100/(BSFC \cdot LCV) \ \ (\%) \quad (3)$$

The repeatability of the three repeats was given as the coefficient of variation (CoV) and the combined uncertainty of the measurements was given as the root-sum-square method of Holman [16]. These are stated in Table 4 along with the propagated uncertainties.

Table 4. Instrument uncertainties and propagated uncertainty of the derived quantities.

Measured quantity	**Uncertainty (%)**	**Derived quantity**	**Uncertainty (%)**
Load (load cell)	±0.20	Brake power	±0.32

Measured quantity	Uncertainty (%)	Derived quantity	Uncertainty (%)
Speed	±0.25	Fuel mass flow	±0.51
Burette time	±0.50	BSFC	±0.60
Fuel density	±0.10	BTE	±0.67
Calorific value	±0.30		
Exhaust gas temperature	±0.40	Overall experiment	±1.92
NOx / CO / HC / CO_2	±1.0 / ±0.6 / ±1.0 / ±0.5		

2.5 Statistical analysis

In the Taguchi stage, the larger-the-better S/N ratio was used for BTE, and the smaller-the-better S/N ratio was used for BSFC and the four emissions.

$$S/N_{LB} = -10 \log_{10}[(1/n) \Sigma 1/y_i^2]; \quad S/N_{SB} = -10 \log_{10}[(1/n) \Sigma y_i^2] \qquad (4)$$

where yi is the i-th repeat and n = 3. The contribution percentages of the individual factors were calculated from the analysis of variance (ANOVA) of the S/N ratios. The six responses were merged by grey relational analysis [15]. The mean responses were normalized to a value from 0 to 1. BTE was the larger-the-better response, while the rest were smaller-the-better responses. The grey relational coefficient of the k-th response in the i-th run was calculated with the distinguishing coefficient of $\zeta = 0.5$.

$$\xi_i(k) = (\Delta_{min} + \zeta\Delta_{max})/(\Delta_i(k) + \zeta\Delta_{max}) \qquad (5)$$

where Δi(k) is the deviation of the normalized value of the ith response from the ideal value of 1. The overall grey relational grade (GRG) was the average of the six coefficients. In the Box-Behnken stage, each of the responses was fitted to a full quadratic model in coded variables x1 (CR), x2 (IP) and x3 (B) by least squares.

$$y = \beta_0 + \Sigma\beta_i x_i + \Sigma\beta_{ii} x_i^2 + \Sigma\Sigma\beta_{ij} x_i x_j \qquad (6)$$

ANOVA tests and the coefficient of determination R2 and adjusted R2 were used to validate the models. Then the GRG was checked on a fine grid of the fitted responses, with the one of maximum grade selected. Analysis for the DEE dosage experiment?was performed using a one-way analysis of variance (ANOVA) followed by Tukey's honestly important difference test at an importance level of 0.05. Property tests were performed using Excel and S/N, ANOVA, response surface and grey relational calculations were made using MATLAB.

III. RESULTS AND DISCUSSION

3.1 Verified baseline for diesel and the blends

The benchmark was determined from the raw burette times at six loads at compression ratio 17 and 200 bar. Table 5 gives the times together with the coefficient of variation, CV, and the BTE for diesel and the three blends at each load. For diesel, the burette time was 86.8 s at 17% load and 30.0 s at full load (CoV of these repeat times was less than 1.7% at every point which indicates that the measurement of the fuel was repeatable). Fig. 3 also shows the BTE and BSFC error bars, which are one standard deviation.

Table 5. Recorded burette times for 10 cm³ of fuel (mean of three repeats), their coefficient of variation and the derived brake thermal efficiency at six loads (CR 17, 200 bar).

Load (%)	Diesel t (s)	CoV (%)	BTE (%)	B10 t (s)	CoV (%)	BTE (%)	B15 t (s)	CoV (%)	BTE (%)	B20 t (s)	CoV (%)	BTE (%)
17	86.8	0.08	14.21	84.1	1.75	13.82	84.1	0.95	13.84	84.2	0.87	13.88

Load (%)	Diesel t (s)	CoV (%)	BTE (%)	B10 t (s)	CoV (%)	BTE (%)	B15 t (s)	CoV (%)	BTE (%)	B20 t (s)	CoV (%)	BTE (%)
33	65.6	1.16	21.65	64.1	0.59	21.25	64.8	0.99	21.50	63.6	0.86	21.15
50	52.3	0.20	25.84	50.9	0.67	25.26	51.6	0.85	25.62	50.5	0.69	25.14
67	43.1	0.66	28.34	42.4	0.23	28.00	42.0	0.59	27.74	41.6	0.78	27.53
83	36.5	0.67	30.10	36.1	0.86	29.86	35.9	0.33	29.77	35.5	0.76	29.44
100	30.0	0.50	29.62	29.6	0.44	29.32	29.4	0.21	29.21	28.7	0.72	28.54

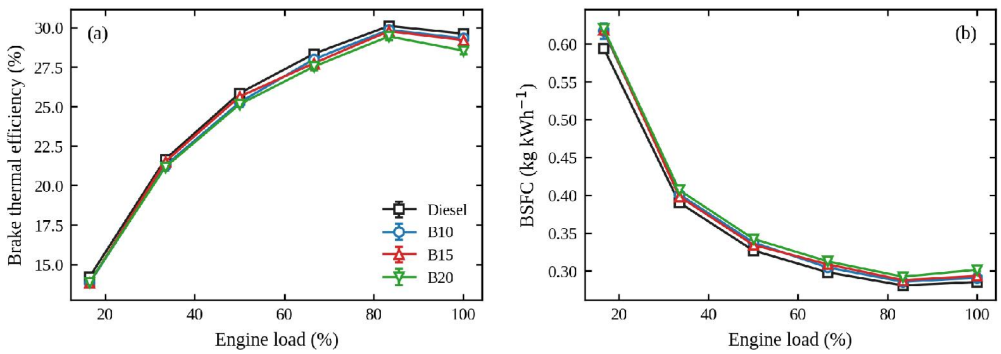

Fig. 3. Baseline (a) brake thermal efficiency and (b) brake specific fuel consumption of diesel, B10, B15 and B20 against engine load at CR 17 and 200 bar. Error bars show one standard deviation of three repeats.

BTE increased with load for all fuels, peaking at 83% load. At this load, BTE reached a highest value of 30.1% for diesel and 29.4% for B20, before again following the diesel curve, with increasing distance between the curves with increasing blend ratio. At 83% load, the BTE of B10, B15 and B20 were lower than diesel by 0.24, 0.33 and 0.66 percentage points, respectively. Differences between B10 and diesel were within the combined uncertainty. B20 was less than diesel above 50% load conditions. In contrast, BSFC increased by 3.9% with B20 at the 83% load condition, likely as a result of its lower energy density and higher viscosity. Blending the biodiesel with diesel resulted in higher fuel injection rates and larger droplet sizes that both adversely affect the combustion characteristics [2,4]. The same penalty was reported by Sahoo and Das [4] for Jatropha and Karanja methyl esters. The slight decrease in full load for all fuels is typical of a naturally aspirated engine, reflecting the fall in air-fuel ratio and a rise in heat loss.

3.2 Screening of the four factors by the Taguchi method

The L16 array of the experiment, the mean of the six responses and the S/N ratios of BTE and NOx as well as the grey relational grade of each run are presented in Table 6. The highest BTE of 30.82% was recorded for run 3 (diesel, 5% DEE, 200 bar, CR 17), while the lowest NOx of 689 ppm was recorded for run 1 (lowest CR and injection pressure). The best performance was obtained at a high compression ratio, a middle injection pressure and a low or moderate blend ratio.

Table 6. Taguchi L16 array with mean responses at 75% load, S/N ratios of BTE and NOx and grey relational grade.

Run	B (%)	DEE (%)	IP (bar)	CR	BTE (%)	BSFC (kg kWh^{-1})	CO (%)	HC (ppm)	CO_2 (%)	NOx (ppm)	S/N BTE (dB)	S/N NOx (dB)	GRG	Rank
1	0	0	180	15	27.38	0.309	0.167	42.8	6.89	689	28.75	-56.76	0.560	10
2	0	3	190	16	29.76	0.285	0.131	34.7	7.40	775	29.47	-57.79	0.597	7

IJARSCT
International Journal of Advanced Research in Science, Communication and Technology
International Open-Access, Double-Blind, Peer-Reviewed, Refereed, Multidisciplinary Online Journal
ISSN: 2581-9429
Volume 6, Issue 1, September 2026
Impact Factor: 8.2

Run	B (%)	DEE (%)	IP (bar)	CR	BTE (%)	BSFC (kg kWh^{-1})	CO (%)	HC (ppm)	CO_2 (%)	NOx (ppm)	S/N BTE (dB)	S/N NOx (dB)	GRG	Ran k
3	0	5	200	17	30.82	0.277	0.114	31.1	7.92	906	29.78	-59.15	0.679	1
4	0	8	210	18	30.59	0.280	0.110	33.3	8.39	1039	29.71	-60.33	0.592	8
5	10	0	190	17	29.71	0.287	0.090	26.3	7.84	1009	29.46	-60.07	0.598	6
6	10	3	180	18	29.32	0.292	0.088	25.3	8.15	1061	29.34	-60.52	0.562	9
7	10	5	210	15	28.43	0.302	0.100	28.2	7.79	825	29.08	-58.33	0.538	11
8	10	8	200	16	29.76	0.290	0.082	28.4	8.17	859	29.47	-58.68	0.605	5
9	15	0	200	18	29.91	0.286	0.081	22.9	8.35	1225	29.52	-61.76	0.619	3
10	15	3	210	17	29.94	0.288	0.071	21.0	8.34	1100	29.53	-60.83	0.678	2
11	15	5	180	16	28.44	0.304	0.093	28.2	7.92	851	29.08	-58.60	0.534	12
12	15	8	190	15	27.75	0.313	0.096	32.6	7.95	765	28.86	-57.67	0.514	15
13	20	0	210	16	28.83	0.299	0.094	26.4	8.10	1086	29.20	-60.72	0.517	13
14	20	3	200	15	27.88	0.310	0.104	29.0	7.86	899	28.91	-59.07	0.491	16
15	20	5	190	18	29.97	0.290	0.078	23.5	8.75	1159	29.53	-61.28	0.608	4
16	20	8	180	17	29.13	0.299	0.085	31.1	8.58	975	29.29	-59.78	0.514	14

Main effects plots (Fig. 4) show the direction and magnitude of each factor: the BTE S/N ratio increases up to CRs of 17 and becomes constant beyond this; the S/N ratio increases with injection pressure up to 200 bar and then decreases slightly at 210 bar. Higher blends eventually dropped the BTE ratio, but DEE improved the BTE ratio only 5% maximum. NOx displayed the opposite trends for compression ratio, injection pressure, and blend ratio, meaning that efficiency improvements came at the cost of higher NOx emissions. DEE was the only case that improved the two ratios at the same time. In addition, the highest values of the global response defined as the grey relational grade, were obtained at CR 17, 200 bar, 5% DEE and B0 or B15.

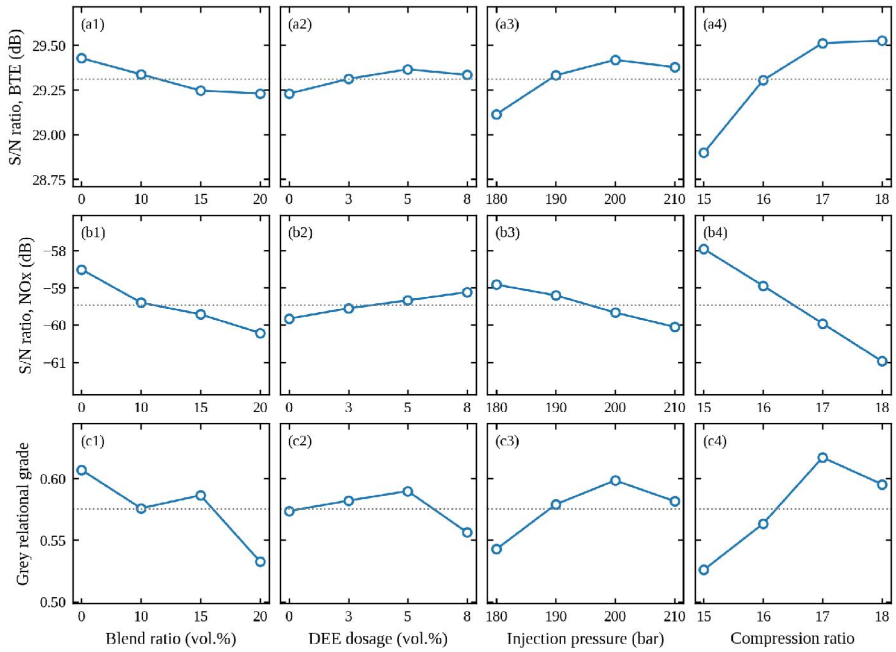

Fig. 4. Main effect plots of (a) the S/N ratio of BTE, (b) the S/N ratio of NOx and (c) the grey relational grade for blend ratio, DEE dosage, injection pressure and compression ratio. Dotted lines show the overall mean.

Table 7. ANOVA of the S/N ratios of BTE and NOx from the L16 array.

Source	DF	SS (BTE)	F	p	Contribution (%)	SS (NOx)	F	p	Contribution (%)
Blend ratio	3	0.0995	15.7	0.024	7.1	6.174	111.0	0.001	20.2
DEE dosage	3	0.0408	6.4	0.080	2.9	1.108	19.9	0.017	3.6
Injection pressure	3	0.2207	34.8	0.008	15.8	3.019	54.3	0.004	9.9
Compression ratio	3	1.0270	162.1	<0.001	73.7	20.222	363.5	<0.001	66.1
Error	3	0.0063	–	–	0.5	0.056	–	–	0.2
Total	15	1.3943	–	–	100.0	30.578	–	–	100.0

Table 7 shows ANOVA results on these effects. Compression ratio accounted for 73.7% of BTE ratio variance and 66.1% of NOx ratio variance, with p-values < 0.001. The second most important factor for BTE was injection pressure at 15.8%, while blend ratio was the second most meaningful factor for NOx with 20.2%. DEE dosage has the least effect on BTE (2.9%) and NOx (3.6%) (but the effect on BTE is statistically insignificant). Grey relational grade gives the same order with weight values 39.6%, 24.6%, 13.8%, and 5.2% for CR, blend ratio, injection pressure, and DEE, respectively. CR, blend ratio, and injection pressure are taken to response surface methodology experiments, and DEE is fixed at 5%, where the BTE S/N ratio is maximum, and the grey relational grade is also maximum. The compression ratio was dominant, which showed consistency with the VCR tests from Muralidharan and Vasudevan [5] and Sayin and Gumus [6]. The high precision of BTE (0.5% residual error) shows that the experimental noise was reproduced well during the three repeats.

IJARSCT
International Journal of Advanced Research in Science, Communication and Technology
International Open-Access, Double-Blind, Peer-Reviewed, Refereed, Multidisciplinary Online Journal
ISSN: 2581-9429
Volume 6, Issue 1, September 2026
Impact Factor: 8.2

3.3 Effect of diethyl ether dosage

Since being the lowest of the screening, the effect of DEE on NOx was evaluated as a one-way experiment with B15, CR 17 and 200 bar. Fig. 5 shows the average NOx, CO and HC emissions at 0, 3, 5 and 8% DEE, with the error bars corresponding to one standard deviation. Table 8 summarizes the ANOVA and Tukey groupings. The reductions in NOx were 3.2%, 5.6% and 7.6% at 3%, 5% and 8% DEE, respectively. A one-way ANOVA produced F = 211.8 ($p < 0.001$). Since all doses were different in Tukey's test, the concomitant decrease in the NOx concentrations is not an artifact.

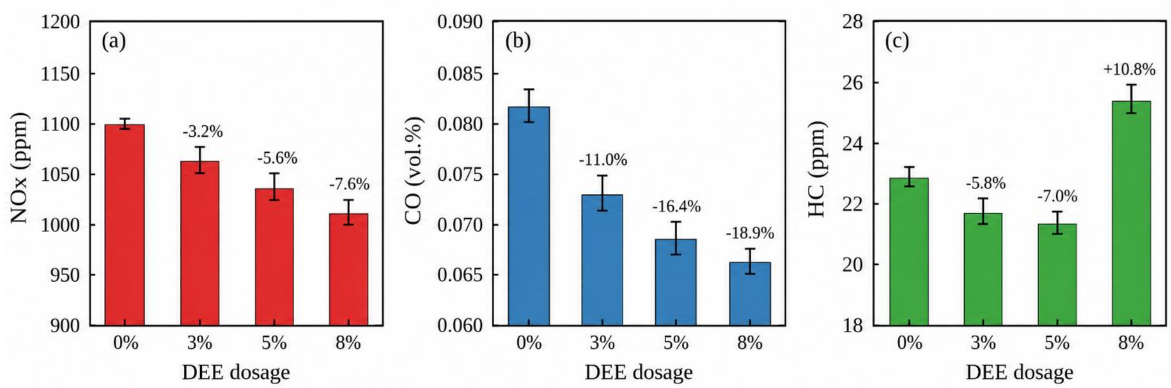

Fig. 5. Effect of DEE dosage on (a) NOx, (b) CO and (c) HC at 75% load for B15, CR 17 and 200 bar. Error bars show one standard deviation of three repeats; labels give the change relative to the plain blend.

Table 8. One-way ANOVA and Tukey groupings for the effect of DEE dosage (B15, CR 17, 200 bar, 75% load).

Response	0% DEE	3% DEE	5% DEE	8% DEE	F (3, 8)	p	Tukey groups
NOx (ppm)	1099	1064	1037	1015	211.8	<0.001	a, b, c, d
CO (vol.%)	0.082	0.073	0.069	0.066	60.3	<0.001	a, b, bc, c
HC (ppm)	22.96	21.63	21.34	25.43	86.6	<0.001	a, b, b, c
BTE (%)	29.59	30.02	30.32	30.24	60.6	<0.001	a, b, c, c
CO_2 (vol.%)	8.09	8.29	8.36	8.57	36.2	<0.001	a, b, b, c

Dosages that share a letter are not significantly different at the 5% level.

CO emissions decreased by 16.4% and 18.9% at 5% and 8% DEE. The BTE increased by 2.4% at 5% DEE, but plateaued afterwards. The NOx and CO trends have a common cause. DEE's high latent heat reduces both charge and peak temperature upon injection and high cetane number of DEE reduces ignition delay and the premixed fraction of heat release [9,11]. Lower temperature from DEE reduces thermal NOx formation. At the same time, more oxygen and less viscosity in the mixture improved the mixing of the fuel and oxidised CO more completely [10]. HC behaved differently. After 3 and 5% DEE it decreased, but increased by 10.8% with 8% DEE. The Tukey test indicated that the 8% DEE was in its own group. This increase at the 8% level is attributed to over cooling of charge and the very low boiling point of DEE resulting in flash vaporization of some fuel and its distribution to cylinder walls and crevices prior to combustion, similar to that observed by Rakopoulos et al. [9]. The 5% dosage was found to give the best NOx, CO and HC balance and was used for future optimization.

3.4 Response surface models

Tables 9 show Box-Behnken responses for compression ratio, injection pressure and blend ratio at 5% DEE. The three centre-point values for BTE and NOx were within 0.5 and 1% respectively, indicating small variability in engine performance repeatability between individual runs. Table 10 shows the coded quadratic models that were fitted, along with the analysis of variance (ANOVA) statistics.

Table 9. Box–Behnken design matrix and mean responses at 75% load with 5% DEE.

Run	CR	IP (bar)	B (%)	BTE (%)	BSFC (kg kWh^{-1})	CO (vol.%)	HC (ppm)	CO_2 (vol.%)	NOx (ppm)
1	16	190	15	29.29	0.295	0.085	25.5	8.05	890
2	18	190	15	30.16	0.286	0.070	22.5	8.58	1120
3	16	210	15	29.45	0.293	0.079	24.3	8.21	972
4	18	210	15	30.20	0.286	0.069	21.0	8.72	1214
5	16	200	10	29.80	0.289	0.083	25.0	7.99	876
6	18	200	10	30.43	0.283	0.073	22.6	8.51	1108
7	16	200	20	29.57	0.293	0.086	24.9	8.30	976
8	18	200	20	30.07	0.288	0.072	22.1	8.82	1198
9	17	190	10	30.08	0.286	0.081	24.5	8.15	941
10	17	210	10	30.42	0.283	0.075	22.4	8.30	1044
11	17	190	20	29.93	0.290	0.078	24.7	8.46	1034
12	17	210	20	29.99	0.289	0.073	22.4	8.65	1132
13	17	200	15	30.35	0.285	0.068	22.0	8.38	1029
14	17	200	15	30.26	0.285	0.069	22.0	8.36	1032
15	17	200	15	30.41	0.284	0.069	21.8	8.34	1038

Table 10. Quadratic response models in coded variables (x1 = (CR − 17)/1, x2 = (IP − 200)/10, x3 = (B − 15)/5) and their ANOVA statistics.

Response	Fitted model	F (9, 5)	p	R^2	Adjusted R^2
BTE (%)	$30.340 + 0.346x_1 + 0.075x_2 - 0.145x_3 - 0.352x_1^2 - 0.214x_2^2 - 0.021x_3^2 - 0.032x_1x_2 - 0.034x_1x_3 - 0.070x_2x_3$	22.0	0.002	0.975	0.930
BSFC (kg kWh^{-1})	$0.2847 - 0.0033x_1 - 0.0007x_2 + 0.0027x_3 + 0.0034x_1^2 + 0.0021x_2^2 + 0.0001x_3^2 + 0.0003x_1x_2 + 0.0003x_1x_3 + 0.0007x_2x_3$	26.5	0.001	0.979	0.942
CO (vol.%)	$0.0689 - 0.0062x_1 - 0.0021x_2 - 0.0004x_3 + 0.0042x_1^2 + 0.0027x_2^2 + 0.0054x_3^2 + 0.0010x_1x_2 - 0.0010x_1x_3 + 0.0001x_2x_3$	55.2	<0.001	0.990	0.971
HC (ppm)	$21.91 - 1.44x_1 - 0.88x_2 - 0.05x_3 + 0.78x_1^2 + 0.64x_2^2 + 0.94x_3^2 - 0.05x_1x_2 - 0.09x_1x_3 - 0.06x_2x_3$	26.1	0.001	0.978	0.940
CO_2 (vol.%)	$8.362 + 0.261x_1 + 0.079x_2 + 0.161x_3 + 0.022x_1^2 + 0.006x_2^2 + 0.020x_3^2 - 0.003x_1x_2 + 0.002x_1x_3 + 0.011x_2x_3$	450.4	<0.001	0.999	0.997
NOx (ppm)	$1033.1 + 115.7x_1 + 47.1x_2 + 46.3x_3 + 8.9x_1^2 + 7.3x_2^2 - 2.5x_3^2 + 3.2x_1x_2 - 2.7x_1x_3 - 0.9x_2x_3$	491.9	<0.001	0.999	0.997

All of these six models were statistically meaningful ($p < 0.01$) and had values of R^2 ranging between 0.975 and 0.999. Moreover, the adj. R^2 were all greater than 0.93, which justified the quadratic terms and indicated that no over-fitting was the case. Fig. 6 shows the calculated and measured values of BTE and NOx are located along the diagonal, and Table 10 presents the coefficients of the calculated responses and their physical modeling. For BTE, the

IJARSCT

International Journal of Advanced Research in Science, Communication and Technology

International Open-Access, Double-Blind, Peer-Reviewed, Refereed, Multidisciplinary Online Journal

ISSN: 2581-9429 Volume 6, Issue 1, September 2026 Impact Factor: 8.2

linear and square x1 (CR) and for NOx the linear are meaningful, but the negative square of x1 gives a maximum within the range of values being tested. The increase of NOx is higher for x1 (compression ratio), with 116 ppm for each unit less than the 47 ppm for the 10 bar increase, and the 5% biodiesel increase of 46 ppm. The interaction terms were small for all responses, suggesting the effects of factors were essentially independent in the range studied.

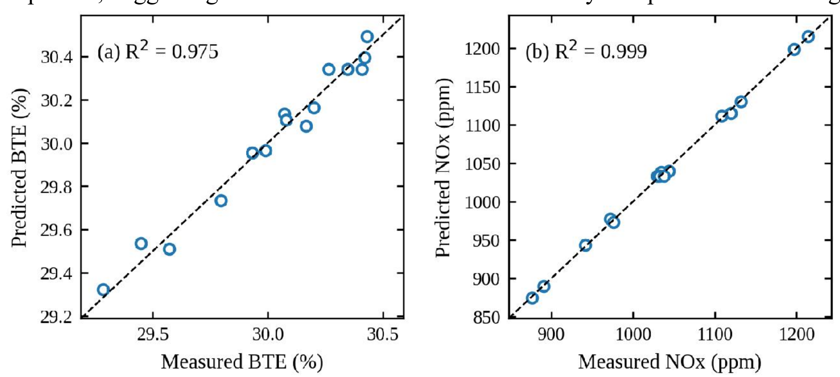

Fig. 6. Predicted against measured values from the Box–Behnken runs for (a) BTE and (b) NOx. The dashed line is the line of equality.

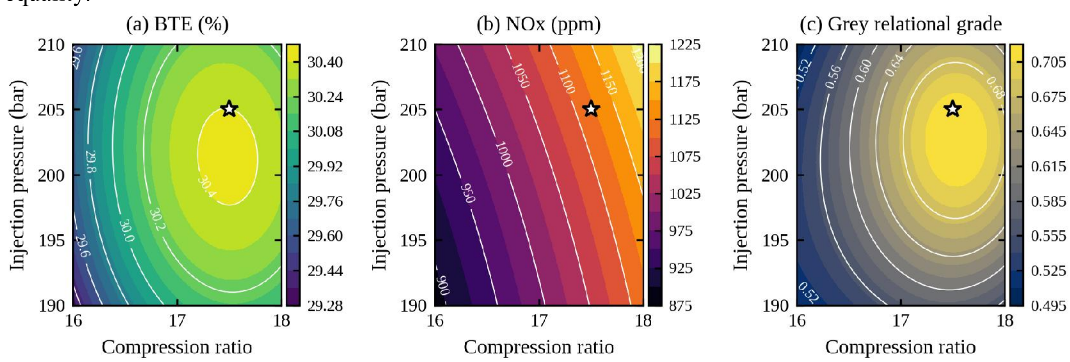

Fig. 7. Contour plots of (a) BTE, (b) NOx and (c) grey relational grade against compression ratio and injection pressure at B15 and 5% DEE. The star marks the selected optimum.

The contour plots in Fig. 7 explain this joint optimum: BTE reaches a maximum at CR 17.5 and injection pressure of 202 bar, and reduces away on both sides because maximum heat transfer losses and friction losses occur at high CR, and decreased mixing occurs due to excessive spray over-penetration at high pressure [6,7]. In contrast, NOx value continually increases throughout the domain, so the grey relational grade in Fig. 7(c) appears to rise in a ridge following the BTE maximum, but pulled a little towards the low CR and pressure direction due to its influence and the CO_2 and BSFC terms. The maximum grade of 0.731 was reached at a compression ratio of 17.5, 203 bar, B13. The nearest practical operating conditions are CR 17.5, 205 bar, B15 and 5% DEE (diesel engine efficiency).

3.5 Confirmation of the optimum and load curves

Table 11. Confirmation runs at the optimum setting (CR 17.5, 205 bar, B15, 5% DEE) at 75% load, compared with diesel and B15 at the standard setting (CR 17, 200 bar).

Response	Predicted	Measured (mean ± SD)	Deviation (%)	Diesel, standard	B15, standard	Change vs diesel (%)	Change vs B15 (%)
BTE (%)	30.40	29.88 ± 0.12	-1.7	30.53	29.85	-2.1	0.1

DOI: 10.48175/IJARSCT-38239

IJARSCT

International Journal of Advanced Research in Science, Communication and Technology

International Open-Access, Double-Blind, Peer-Reviewed, Refereed, Multidisciplinary Online Journal

ISSN: 2581-9429 Volume 6, Issue 1, September 2026 Impact Factor: 8.2

Response	Predicted	Measured (mean ± SD)	Deviation (%)	Diesel, standard	B15, standard	Change vs diesel (%)	Change vs B15 (%)
BSFC (kg kWh^{-1})	0.284	0.281 ± 0.001	-1.2	0.276	0.288	1.8	-2.5
CO (vol.%)	0.067	0.065 ± 0.001	-1.9	0.126	0.081	-48.3	-19.1
HC (ppm)	21.1	20.8 ± 0.6	-1.3	33.1	24.0	-37.1	-13.1
CO_2 (vol.%)	8.54	8.70 ± 0.05	1.9	7.58	8.02	14.8	8.4
NOx (ppm)	1119	1108 ± 2	-1.0	966	1098	14.6	0.9

Three design value confirmation runs are summarized in Table 11, and compared to the model predictions. For all six response variables, there are differences of less than 2%, below the design acceptance limit of 5%. Optimum BTE was 29.88%, 0.1% higher than the baseline B15 and 2.1% lower than diesel. CO and HC were 48% and 37% lower than diesel. NOx was 14.6% higher than diesel. The NOx was only 0.9% higher than the modest B15 blend, so virtually offsetting the NOx had been achieved with the improved compression ratio and pressure with the penalty of higher NOx as the only downside, versus the benefits of the combined optimization.

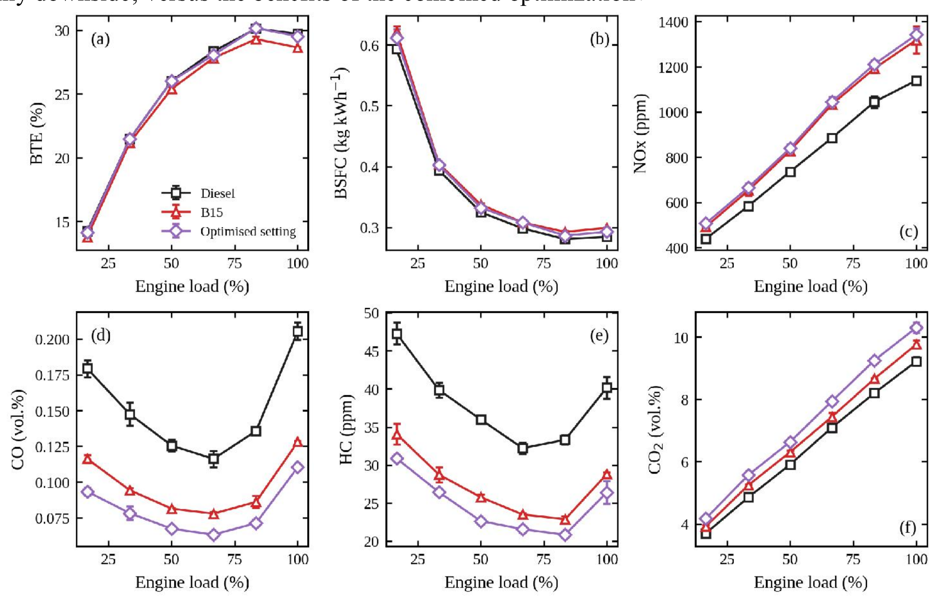

Fig. 8. Load curves of (a) BTE, (b) BSFC, (c) NOx, (d) CO, (e) HC and (f) CO_2 for diesel and B15 at the standard setting and for the optimised setting (CR 17.5, 205 bar, B15, 5% DEE). Error bars show one standard deviation of three repeats.

This is confirmed in Fig. 8, as the optimized setting met or exceeded the diesel BTE at each load and was 0.86 percentage points higher than B15 at the 83% load point. The BSFC is between the two reference fuels as the improved conversion efficiency countered the lower calorific value of the blend. The CO and total HC were lowest for the optimized setting across the load range. CO was reduced by -45.6% at 67% load, and total HC by -33.1%. At full load operation where the mixture is richest there was an increase in CO across all fuels, with the optimized setting still -46% lower than diesel. In NOx, all fuels exhibited near-linear behavior with load, NOx emissions were higher than the reference diesel in both biodiesel cases. The optimized curve was in error bars to B15. CO_2 was also highest for the optimized setting, indicating more complete combustion. Taken together these load curves show that the optimum found at 75% load holds across the range of working load for the engine. These results support the Datta and Mandal [3] proposal that engine side adjustment and oxygenated additives are complementary solutions to using biodiesel with no engine performance penalty and add a verified, statistically tested operating setting for a VCR engine.

IV. CONCLUSION

This research study investigates the optimization of the blend ratio, DEE dosage, injection pressure and compression ratio together on a single cylinder VCR diesel engine using a four stage design programme with three repeats at each parametric point. The details are as follows.

(1) An accurate baselined raw burette, with BTE decreasing and BSFC increasing with blend ratio. B10 was within the measurement error of ±0.67% and B20 was 0.66 percentage points lower than diesel at 83% load.

(2) For the second response (SY2), compression ratio was the most important factor for BTE SNR and NOx (73.7% and 66.1% respectively), followed by injection pressure and blend ratio. DEE dosage was the least meaningful contributor, with less than 4% contribution to either response.

(3) Compared to control, NOx and CO emissions decreased by ~5.6% and ~16.4% respectively at 5% DEE, both statistically important in Tukey. HC emissions increased by 10.8% under 8% DEE. Thus, 5% DEE can be recommended.

(4) With adjusted R^2 above 0.93, the quadratic response models indicated a joint optimum of CR 17.5, 205 bar, B15 and 5% DEE. Confirmation runs were within 2% of optimum for all six responses.

(5) The engine recovered its diesel efficiency (29.88% at 75% load) but the CO and HC were 48% and 37% lower than diesel, respectively, and the NOx was always within 0.9% of the plain B15 blend in the entire range of loads.

The method may be extendable to other feedstocks and additives. More work also needs to take into account the effects on injection timing and exhaust gas recirculation, which have a direct influence on the mechanism of NOx formation, and on combustion pressure, so that heat release can be linked to the results.

Declaration of competing interest

The authors declare that they have no known competing financial interests or personal relationships that could have appeared to influence the work reported in this paper.

Data availability

The data sheets and the spreadsheet file used for data reduction are available upon request from the corresponding author.

REFERENCES

[1] A.K. Agarwal, Biofuels (alcohols and biodiesel) applications as fuels for internal combustion engines, Prog. Energy Combust. Sci. 33 (3) (2007) 233–271. https://doi.org/10.1016/j.pecs.2006.08.003

[2] M. Lapuerta, O. Armas, J. Rodríguez-Fernández, Effect of biodiesel fuels on diesel engine emissions, Prog. Energy Combust. Sci. 34 (2) (2008) 198–223. https://doi.org/10.1016/j.pecs.2007.07.001

[3] A. Datta, B.K. Mandal, A comprehensive review of biodiesel as an alternative fuel for compression ignition engine, Renew. Sustain. Energy Rev. 57 (2016) 799–821. https://doi.org/10.1016/j.rser.2015.12.170

[4] P.K. Sahoo, L.M. Das, Combustion analysis of Jatropha, Karanja and Polanga based biodiesel as fuel in a diesel engine, Fuel 88 (6) (2009) 994–999. https://doi.org/10.1016/j.fuel.2008.11.012

[5] K. Muralidharan, D. Vasudevan, Performance, emission and combustion characteristics of a variable compression ratio engine using methyl esters of waste cooking oil and diesel blends, Appl. Energy 88 (11) (2011) 3959–3968. https://doi.org/10.1016/j.apenergy.2011.04.014

[6] C. Sayin, M. Gumus, Impact of compression ratio and injection parameters on the performance and emissions of a DI diesel engine fueled with biodiesel-blended diesel fuel, Appl. Therm. Eng. 31 (16) (2011) 3182–3188. https://doi.org/10.1016/j.applthermaleng.2011.05.044

[7] V. Hariram, R. Vagesh Shangar, Influence of compression ratio on combustion and performance characteristics of direct injection compression ignition engine, Alexandria Eng. J. 54 (4) (2015) 807–814. https://doi.org/10.1016/j.aej.2015.06.007

[8] S. Kumar, J.H. Cho, J. Park, I. Moon, Advances in diesel–alcohol blends and their effects on the performance and emissions of diesel engines, Renew. Sustain. Energy Rev. 22 (2013) 46–72. https://doi.org/10.1016/j.rser.2013.01.017

[9] D.C. Rakopoulos, C.D. Rakopoulos, E.G. Giakoumis, A.M. Dimaratos, Studying combustion and cyclic irregularity of diethyl ether as supplement fuel in diesel engine, Fuel 109 (2013) 325–335. https://doi.org/10.1016/j.fuel.2013.01.012

[10] S. Sivalakshmi, T. Balusamy, Effect of biodiesel and its blends with diethyl ether on the combustion, performance and emissions from a diesel engine, Fuel 106 (2013) 106–110. https://doi.org/10.1016/j.fuel.2012.12.033

[11] A. Ibrahim, Investigating the effect of using diethyl ether as a fuel additive on diesel engine performance and combustion, Appl. Therm. Eng. 107 (2016) 853–862. https://doi.org/10.1016/j.applthermaleng.2016.07.061

[12] T. Ganapathy, K. Murugesan, R.P. Gakkhar, Performance optimization of Jatropha biodiesel engine model using Taguchi approach, Appl. Energy 86 (11) (2009) 2476–2486. https://doi.org/10.1016/j.apenergy.2009.02.008

[13] M. Pandian, S.P. Sivapirakasam, M. Udayakumar, Investigation on the effect of injection system parameters on performance and emission characteristics of a twin cylinder compression ignition direct injection engine fuelled with pongamia biodiesel–diesel blend using response surface methodology, Appl. Energy 88 (8) (2011) 2663–2676. https://doi.org/10.1016/j.apenergy.2011.01.069

[14] J.B. Hirkude, A.S. Padalkar, Performance optimization of CI engine fuelled with waste fried oil methyl ester-diesel blend using response surface methodology, Fuel 119 (2014) 266–273. https://doi.org/10.1016/j.fuel.2013.11.039

[15] J.L. Deng, Introduction to grey system theory, J. Grey Syst. 1 (1) (1989) 1–24.

[16] J.P. Holman, Experimental Methods for Engineers, eighth ed., McGraw-Hill, New York, 2012